Turkish Journal of Electrical Engineering & Computer Sciences

http://journals.tubitak.gov.tr/elektrik/

Research Article

Turk J Elec Eng & Comp Sci
(2016) 24: 5183 – 5194

doi:10.3906/elk-1504-226

Effect of load increase and power system stabilizer on stability delay margin of a generator excitation control system

Şahin SÖNMEZ, Saffet AYASUN*
Department of Electrical and Electronics Engineering, Niğde University, Niğde, Turkey

Received: 27.04.2015 • **Accepted/Published Online:** 03.11.2015 • **Final Version:** 06.12.2016

Abstract: This paper studies the impact of load increase and a power system stabilizer (PSS) on the stability delay margin of a single-machine-infinite-bus system including an automatic voltage regulator. An analytical method is proposed to determine the stability delay margin of the excitation control system. The proposed method first eliminates transcendental terms in the characteristic equation of the excitation system without making any approximation and transforms the transcendental characteristic equation into a regular polynomial. The key result of the elimination process is that the real roots of the new polynomial correspond to the imaginary roots of the transcendental characteristic equation. With the help of the new polynomial, it is also possible to determine the delay dependency of system stability and the root tendency with respect to the time delay. Delay margins are computed for various loading conditions and PSS gains. It is observed that the delay margin generally decreases as the PSS gain and load demand increase, resulting in a less stable system.

Key words: Generator excitation control, power system stabilizer, time delay, stability, delay margin

1. Introduction

This paper investigates the impact of load increase and power system stabilizer (PSS) on the time delay margin of generator excitation control system. The phasor measurement units (PMUs) and open communication networks have been extensively used in wide-area measurement/monitoring systems. This causes inevitable time delays, which include measurement and communication delays [1,2]. Such time delays may reduce the control system damping performance and could even cause instability if they exceed the upper bound or delay margin for stability [3–5]. Therefore, large time delays must be taken into account in stability analysis and controller design, and practical methods that enable us to determine delay margins should be developed.

In electrical power systems, each generator is equipped with a load frequency control (LFC) system and an automatic voltage regulator (AVR) to keep the system frequency and generator output voltage magnitude at a desirable range when changes are observed in real/reactive load demands [6–8]. Figure 1 shows the one-line diagram of the SMIB system that includes both the AVR and PSS, and Figure 2 illustrates its block diagram with a time delay block in the voltage feedback loop [8].

*Correspondence: sayasun@nigde.edu.tr

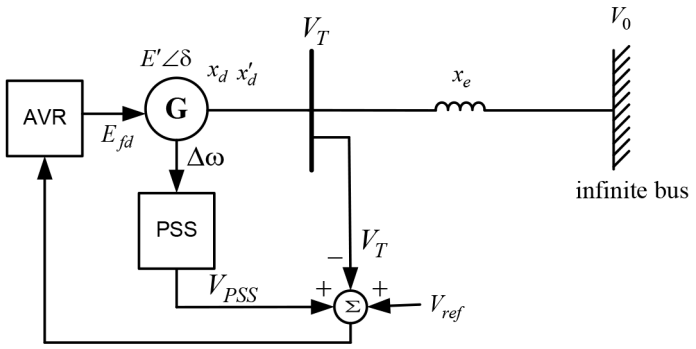

Figure 1. One-line diagram of SMIB with AVR and PSS [8,28].

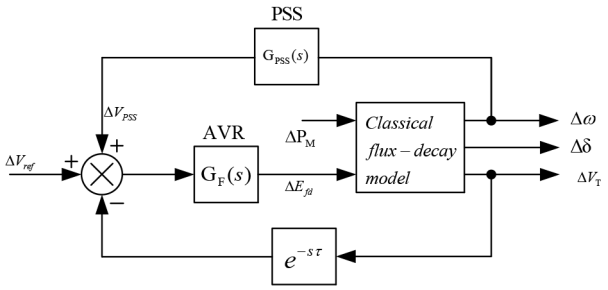

Figure 2. Block diagram of the SMIB system with AVR and PSS [8,28].

Time delays observed in power systems consist of measurement and communication delays. The use of PMUs causes measurement delays, including voltage transducer delay and processing delay. The processing delay is the amount of time required in converting transducer data into phasor information with the help of the discrete Fourier transform (DFT) [1,9]. In power system control, the total measurement delay is reported to be on the order of milliseconds [1–3]. The total communication delays, especially in multiarea LFC systems, can vary from 10 to several hundred milliseconds [10–12]. There are several factors that affect the size of communication delays. These include communication means such as fiber-optic cables, power line carriers, telephone lines, etc., and phasor package size, transmission protocol used, and network load.

This work primarily aims to investigate how the load increase and addition of a PSS will affect the delay margin of the SMIB with AVR and focuses on the time delay observed in the terminal voltage feedback loop, shown as exponential block $e^{-s\tau}$ in Figure 2. It must be stated here that there will be a certain amount of time delay (τ_1) in the PSS loop. This delay may or may not be equal to the delay in the voltage control loop. The inclusion of the delay in the PSS loop will result in another exponential term ($e^{-s\tau_1}$) in the characteristic equation. In this case, the characteristic equation will include incommensurate delay terms like $e^{-s\tau}$ and $e^{-s\tau_1}$ when $\tau_1 \neq \tau$ and commensurate delay terms like $e^{-s\tau}$ and $e^{-s(2\tau)}$ when $\tau_1 = \tau$. Delay margin computation of such a characteristic equation, including commensurate and incommensurate delay terms, is a difficult task and requires a significant amount of computational effort. Therefore, the delay in the PSS loop was neglected in this study to simplify the delay margin computation and to investigate the effect of the single voltage measurement delay on the dynamics of voltage control.

There are several methods for computing delay margins for stability of time-delayed dynamical systems. These methods can be grouped into 2 main types, namely frequency-domain direct and time-domain indirect methods. The main goal of frequency domain approaches is to compute all critical purely imaginary roots of

the characteristic equation for which the system will be marginally stable [13–15]. The frequency domain direct methods can obtain accurate delay margins for constant delays. However, they cannot be applied to stability analysis of time-delayed systems that include time-varying delays. This is a drawback of such methods. The indirect time-domain method utilizes the Lyapunov stability theory and linear matrix inequalities technique [16–18]. Such methods have been applied to estimate the delay margins of the wide-area damping controller [12,19] and LFC systems [11]. These methods can deal with both constant and time-varying delays. However, their delay margin results are more conservative as compared with ones obtained by frequency-domain direct methods [11,20]. Our previous studies clearly indicated that the direct method reported in [13] correctly estimated the delay margins of a generator excitation control system with a constant single delay [4,5], delay margins of load frequency control systems with constant communication delays [20], and a time-delayed DC motor speed control system [21]. In addition to these applications, this frequency-domain direct method was successfully applied to investigate the stability of other time-delayed systems such as mechanical systems [22–24], predator–prey systems [25,26], and a logistic model [27]. Such successful applications, together with correct estimation of delay margins, have motivated us to apply this method to a SMIB system with AVR and PSS.

The proposed method first eliminates exponential terms in the characteristic equation of the SMIB system without making any approximation and transforms the transcendental characteristic equation into a regular polynomial. The key result of the elimination process is that the real roots of the new polynomial correspond to the critical imaginary roots of the transcendental characteristic equation exactly. With the help of the new polynomial, it is also possible to determine the delay dependency of system stability and root tendency with respect to the time delay. An analytical formula is then derived to compute delay margins. The effect of load increase and PSS gain is investigated, and it is found that delay margin generally decreases as the PSS gain and load increase, indicating a less stable system.

2. Single-machine infinite bus system model

For delay margin computation, a linearized model of the SMIB system is required. Figure 3 shows the block diagram of the linearized flux-decay model with a fast exciter [8,28]. The expression for the parameters $K_1 - K_6$ can be found in [8]. Figure 4 illustrates the block diagram of the PSS that includes gain, washout filter, and lead-lag compensator [7,8,28,29]. The basic function of the PSS is to increase the stability limits by modulating

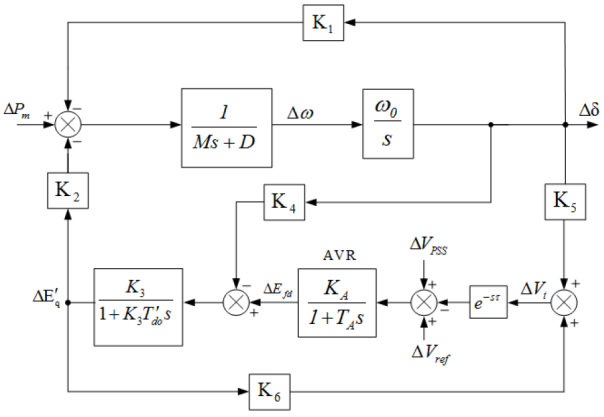

Figure 3. Detailed block diagram of the SMIB system with AVR including a time delay [8,28].

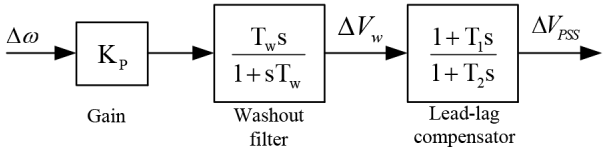

Figure 4. Block diagram of PSS [7,8,28].

the generator excitation to support damping for the rotor oscillations of synchronous machines. Using Figures 2–4, a time-delayed state-space equation model of the system could be easily obtained as

$$\dot{x}(t) = A_0 x(t) + A_\tau x(t-\tau) + Bu(t), \tag{1}$$

where $x(t) = \left[\begin{array}{cccccc} \Delta\delta & \Delta\omega & \Delta E'_q & \Delta E_{fd} & \Delta V_w & \Delta V_{PSS} \end{array} \right]^T$ defines the state variable vector. The meaning of the state variables can be found in [8]. The system matrices are given as

$$A_0 = \begin{bmatrix} 0 & \omega_0 & 0 & 0 & 0 & 0 \\ -\frac{K_1}{M} & -\frac{D}{M} & -\frac{K_2}{M} & 0 & 0 & 0 \\ -\frac{K_4}{T'_{d0}} & 0 & -\frac{K_3}{T'_{d0}} & \frac{1}{T'_{d0}} & 0 & 0 \\ 0 & 0 & 0 & -\frac{1}{T_A} & 0 & \frac{K_A}{T_A} \\ -\frac{K_P K_1}{M} & -\frac{K_P D}{M} & -\frac{K_P K_2}{M} & 0 & -\frac{1}{T_w} & 0 \\ -\frac{K_P K_1 T_1}{M T_2} & -\frac{K_P D T_1}{M T_2} & -\frac{K_P K_2 T_1}{M T_2} & 0 & \left(\frac{1}{T_2} - \frac{T_1}{T_2 T_w}\right) & -\frac{1}{T_2} \end{bmatrix};$$

$$A_\tau = \begin{bmatrix} 0 & 0 & 0 & 0 & 0 & 0 \\ 0 & 0 & 0 & 0 & 0 & 0 \\ 0 & 0 & 0 & 0 & 0 & 0 \\ -\frac{K_A K_5}{T_A} & 0 & -\frac{K_6 K_A}{T_A} & 0 & 0 & 0 \\ 0 & 0 & 0 & 0 & 0 & 0 \\ 0 & 0 & 0 & 0 & 0 & 0 \end{bmatrix}; B = \left[\begin{array}{cccccc} 0 & 0 & 0 & 0 & 0 & \frac{K_A}{T_A} \end{array} \right]^T.$$

3. Delay margin computation

For stability analysis and delay margin computation, it is required to determine the characteristic equation of Eq. (1). This could easily be obtained by using the following:

$$\Delta(s,\tau) = \det(sI - A_0 - A_\tau e^{-s\tau}) = P(s) + Q(s)e^{-s\tau} = 0, \tag{2}$$

where τ the total is time delay, and $P(s)$ and $Q(s)$ are polynomials in s with real coefficients given below:

$$\begin{aligned} P(s) &= p_6 s^6 + p_5 s^5 + p_4 s^4 + p_3 s^3 + p_2 s^2 + p_1 s + p_0 \\ Q(s) &= q_4 s^4 + q_3 s^3 + q_2 s^2 + q_1 s + q_0 \end{aligned}.$$

It must be noted that all the coefficients of the polynomial above will depend on the system parameters. The expressions for coefficients $p_0 - p_6$ and $q_0 - q_4$ are given in the Appendix.

The main purpose of the stability analysis of time-delayed systems is to obtain conditions on the delay for any given set of system parameters that will ensure the stability of the system and to compute the delay margin for stability. Depending on the system parameters, a time-delayed system could be delay-independent or delay-dependent stable. For delay-independent stability, the system remains stable for all finite values of time delay. In a delay-dependent stability case, asymptotic stability holds for $\tau < \tau^*$, where τ represents the delay and τ^* is the critical delay, called the delay margin. If the delay exceeds the margin $\tau > \tau^*$, the system becomes unstable. It is well known that all the roots of the characteristic Eq. (2) must be located

in the left half of the complex plane for a stable system. The characteristic Eq. (2) clearly indicates that $\Delta(s,\tau)=0$ is an implicit function of s and τ. For simplicity, it is assumed that a delay-free ($\tau=0$) system is stable. In other words, all the roots of $\Delta(s,0)=0$ are in the left half-plane. This is a realistic assumption, since a delay-free excitation control system is stable for practical values of the parameters. Suppose that the characteristic equation $\Delta(s,\tau)=0$ has a root on the imaginary axis at $s=j\omega_c$ (where subscript c refers to "crossing" the imaginary axis) for some finite values of the time delay τ. Because of the complex conjugate symmetry of complex roots, the equation $\Delta(-s,\tau)=0$ will also have the same root at $s=j\omega_c$ for the same value of the time delay τ. Consequently, the problem is now reduced to finding values of time delay τ such that both $\Delta(s,\tau)=0$ and $\Delta(-s,\tau)=0$ have a common root at $s=j\omega_c$. This result could be stated as follows:

$$\begin{aligned} P(j\omega_c)+Q(j\omega_c)e^{-j\omega_c\tau}&=0\\ P(-j\omega_c)+Q(-j\omega_c)e^{j\omega_c\tau}&=0 \end{aligned}\quad . \tag{3}$$

By eliminating the exponential terms in Eq. (3), the following new polynomial in ω_c^2 is obtained:

$$\begin{aligned} W(\omega_c^2) &= P(j\omega_c)P(-j\omega_c)-Q(j\omega_c)Q(-j\omega_c)=0\\ &= t_{12}\omega_c^{12}+t_{10}\omega_c^{10}+t_8\omega_c^8+t_6\omega_c^6+t_4\omega_c^4+t_2\omega_c^2+t_0=0 \end{aligned}\quad , \tag{4}$$

where

$$\begin{aligned} &t_{12}=p_6^2; t_{10}=p_5^2-2p_6p_4;\\ &t_8=p_4^2-q_4^2-2p_5p_3+2p_2p_6;\\ &t_6=p_3^2-q_3^2-2p_6p_0+2p_5p_1-2p_4p_2+2q_4q_2;\\ &t_4=p_2^2-q_2^2+2p_4p_0-2p_3p_1-2q_0q_4+2q_3q_1;\\ &t_2=p_1^2-q_1^2-2p_2p_0+2q_2q_0; t_0=p_0^2-q_0^2; \end{aligned}\quad .$$

It must be noted that the characteristic equation with an exponential term given in Eq. (2) is now transformed into a regular polynomial not including any exponential terms given by Eq. (4). The positive real roots of Eq. (4) correspond to the imaginary roots of Eq. (2) exactly. One could easily compute these real roots by standard methods. Depending on the roots of Eq. (4), the following situations might be observed [13]:

1. The polynomial of Eq. (4) does not include any positive real roots. This implies that the characteristic equation of Eq. (2) does not contain any roots on the $j\omega$-axis. Therefore, the excitation control system is delay-independent stable for all finite delays $\tau\geq 0$;

2. The polynomial of Eq. (4) may have at least 1 positive real root. This implies that the characteristic equation of Eq. (2) contains at least a pair of complex roots on the $j\omega$-axis. Thus, the excitation control system is delay-dependent stable.

For a positive real root ω_c of Eq. (4), the delay margin τ^* could be computed using Eq. (3) as follows [5,13]:

$$\begin{aligned} &\tau^*=\tfrac{1}{\omega_c}Tan^{-1}\left(\tfrac{a_9\omega_c^9+a_7\omega_c^7+a_5\omega_c^5+a_3\omega_c^3+a_1\omega_c}{a_{10}\omega_c^{10}+a_8\omega_c^8+a_6\omega_c^6+a_4\omega_c^4+a_2\omega_c^2}\right)+\tfrac{2r\pi}{\omega_c};\\ &r=0,1,2,.....,\infty \end{aligned} \tag{5}$$

where

$$a_{10} = p_6q_4; a_9 = p_5q_4 - p_6q_3; a_8 = p_5q_3 - p_4q_4 - p_6q_2;$$
$$a_7 = p_4q_3 + p_6q_1 - p_3q_4 - p_5q_2;$$
$$a_6 = p_6q_0 + p_4q_2 + p_2q_4 - p_5q_1 - p_3q_3;$$
$$a_5 = p_5q_0 + p_3q_2 + p_1q_4 - p_4q_1 - p_2q_3;$$
$$a_4 = p_1q_3 + p_3q_1 - p_4q_0 - p_2q_2 - p_0q_4;$$
$$a_3 = p_0q_3 - p_3q_0 - p_1q_2 + p_2q_1; a_2 = p_2q_0 + p_0q_2 - p_1q_1;$$
$$a_1 = p_1q_0 - p_0q_1; a_0 = -p_0q_0$$

For any positive roots of Eq. (4), we should also investigate if at $s = j\omega_c$, the root of Eq. (2) crosses the imaginary axis with increasing τ. The necessary condition for the existence of roots crossing the imaginary axis is that the critical characteristic roots cross the imaginary axis with a nonzero velocity defined as follows:

$$Re\left[\frac{ds}{d\tau}\right]_{s=j\omega_{ck}} \neq 0, \tag{6}$$

where $Re(\bullet)$ represents the real part of a complex variable. The sign of root sensitivity is defined as root tendency (RT) [5,13,15]:

$$RT|_{s=j\omega_c} = sgn\left\{Re\left[\frac{ds}{d\tau}\right]_{s=j\omega_c}\right\} = sgn\left[W'(\omega_c^2)\right], \tag{7}$$

where the prime represents differentiation with respect to ω_c^2. The derivation of Eq. (7) could be found in [5]. The RT expression gives a practical tool to evaluate the direction of transition of the roots at $s = j\omega_c$ as τ increases from $\tau_1 = \tau^* - \Delta\tau$ to $\tau_2 = \tau^* + \Delta\tau$, $0 < \Delta\tau << 1$. The root $s = j\omega_c$ crosses the imaginary axis to either the unstable right half-plane when $RT = +1$ or to the stable left half-plane when $RT = -1$. For the excitation control system, by applying Eq. (7), we obtain the following equation that allows us to compute the RT for each crossing frequency:

$$W'(\omega_c^2) = 6t_{12}\omega_c^{10} + 5t_{10}\omega_c^8 + 4t_8\omega_c^6 + 3t_6\omega_c^4 + 2t_4\omega_c^2 + t_2. \tag{8}$$

Another frequency domain method known as Rekasius substitution [14,15] could also be used to compute the delay margins of the SMIB system. This method also eliminates the exponential term $e^{-s\tau}$ in the characteristic equation of Eq. (2) by using an exact substitution given by

$$e^{-s\tau} = \frac{1 - Ts}{1 + Ts}, \tag{9}$$

where $T \in \Re$ is called the pseudo-delay. Using this substitution, the transcendental characteristic Eq. (2) is converted into a polynomial without transcendentality similar to the one given in Eq. (4) such that its purely imaginary roots, determined by the Routh–Hurwitz stability criterion, coincide with the purely imaginary roots of the characteristic Eq. (2) exactly. The corresponding delay margin is then determined by the following formula [15]:

$$\tau^* = \frac{2}{\omega_c}\left[Tan^{-1}(\omega_c T) \pm r\pi\right], \; r = 0, 1, 2, \ldots \tag{10}$$

It must be noted that both the proposed method [13] and the Rekasius substitution method [15] eliminate the transcendental term in the characteristic Eq. (2) using different substitutions that are both exact and obtain a new polynomial without transcendentality. In the proposed method, the real roots of this new polynomial, if they exist, coincide with the imaginary roots $s = \pm j\omega$ of the characteristic equation exactly. As compared to the proposed method, the Rekasius substitution method requires the introduction of a pseudo-delay (T) and an additional step, which is the Routh–Hurwitz stability criterion, to determine the pseudo-delay T and the imaginary roots of the characteristic equation. Therefore, the Rekasius substitution method is not a computationally attractive method when there is a single time delay term in the characteristic equation. Moreover, our previous studies [20,30] on the stability of the time-delayed LFC systems clearly indicated that the Rekasius substitution method gives the same delay margin results as the proposed method since they are both exact methods. However, the proposed method cannot be used when independent unequal time delays are observed in the PSS loop and voltage control loop. Such a delay situation is known as an incommensurate delays case, and recent studies on the Rekasius substitution method show that this method could be extended to delay margin computation of systems with multiple incommensurate delays [31,32].

4. Results

Case studies are performed for the SMIB system shown in Figure 1. Delay margins are computed for various PSS gains in the range of $K_P = 0 - 30$ and load values ranging from $P_L = 0.1pu$ to $P_L = 1.0pu$. The damping is chosen as $D = 0$. The power factor of the load remains unchanged at $pf = \cos\phi = 0.9$ lagging during the load variation. Other system parameters are as follows: $x_d = 1.60$ pu, $x_q = 1.55$ pu, $x'_d = 0.32$ pu, $M = 6.0$, $T'_{do} = 6.0$ s, $\omega_0 = 377 rad/s$, $K_A = 50$, $T_A = 0.05$ s, $T_1 = 0.5$ s, $T_2 = 0.1$ s, $T_w = 2.0$ s, $r_e = 0$, $x_e = 0.4$ pu.

The variation of delay margin with respect to PSS gain for 3 different values of load ($P_L = 0.1, 0.3$, and $0.5pu$) is shown in Figure 5. It is obvious that the impact of PSS gain on the delay margin has 2 tendencies. For small gains, the delay margin increases as the gain increases. This implies that the addition of PSS into the excitation system improves system stability, since the delay margin increases for smaller gains. However, for larger gains, the delay margin decreases as the gain increases, causing a less stable system. Delay margin results are also presented in the Table for these load values. It must be mentioned here that the new characteristic Eq. (4) has 3 real positive roots at each load level. For this reason, delay margins for all 3 real roots are computed using Eq. (5) and presented in the Table. The minimum of 3 delay margins, shown in bold in the Table, is the system delay margin. It is clear from the Table that the delay margin decreases for all values of PSS gain as the load increases, indicating a less stable system.

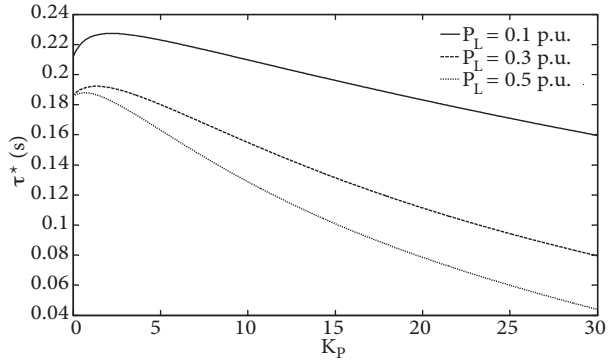

Figure 5. Variation of delay margin with respect to the PSS gain for different loads.

Table. Delay margin with respect to load increase and PSS gain.

$\tau(s)$	P_L (pu)		
	0.1	0.3	0.5
$K_P = 0$	0.2023	0.1789	0.1788
	0.6263	0.5477	0.4579
	0.3138	0.3518	0.3678
$K_P = 5$	0.2230	0.1801	0.1632
	0.4848	0.4303	0.3774
	0.3525	0.4039	0.4262
$K_P = 10$	0.2098	0.1549	0.1289
	0.4580	0.3945	0.3539
	0.3652	0.4247	0.4508
$K_P = 15$	0.1962	0.1315	0.1010
	0.4402	0.3735	0.3407
	0.3764	0.4440	0.4738
$K_P = 20$	0.1832	0.1114	0.0786
	0.4260	0.3592	0.3320
	0.3867	0.4623	0.4958
$K_P = 25$	0.1710	0.0943	0.0600
	0.4141	0.3488	0.3258
	0.3964	0.4799	0.5171
$K_P = 30$	0.1596	0.0796	0.0439
	0.4038	0.3408	0.3214
	0.4056	0.4970	0.5378

Figure 6 shows the variation of delay margin with respect to the load for 3 different values of PSS gain, $K_P = 15$, 20, *and* 25. Note that an increase in load results in a decrease in the delay margin for all PSS gains. Delay margin curves shown in Figure 6 will enable us to determine how much the load could be increased for a given delay such that the system preserves stability. For example, suppose that the maximum amount of delay observed in the system is 0.1 s. From the delay curve shown in Figure 6 for $K_P = 15$, the corresponding amount of load is then found to be $P_L = 0.51pu$. This is the maximum loading point for stability. If the load is further increased, the system will be unstable since the delay observed in the system becomes larger than the delay margin. Evidently, the system will be stable for all selected load values if the delay is ignored in the system. As a result, it is obvious that the delay reduces the maximum loadability of the system and the stability margin.

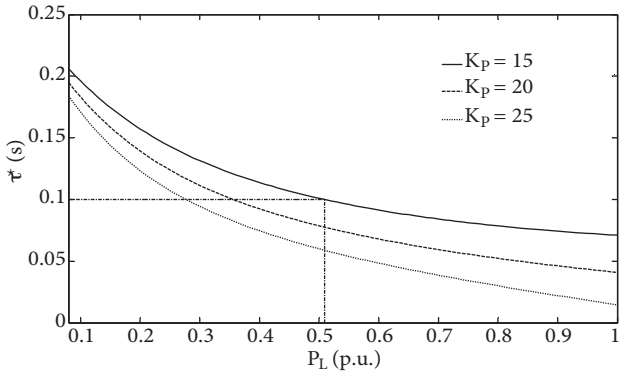

Figure 6. Variation of delay margin with respect to the load for different PSS gains.

The region under the delay curves could be considered as the stability region containing the pairs of time delay and load (τ, P_L), for which the excitation system is stable.

Finally, using MATLAB/Simulink [33], time-domain simulations are carried out to verify the theoretical delay margin results. Figure 7 shows the simulation model in Simulink. For simulation, load and PSS gain are selected as $P_L = 0.5pu$, $K_P = 20$. The constant parameters $K_1 - K_6$ computed are given as: $K_1 = 1.0058$, $K_2 = 0.8441$, $K_3 = 0.36$, $K_4 = 1.0805$, $K_5 = 0.0468$, $K_6 = 0.4991$. For this case, the new characteristic equation in Eq. (4) has 3 real positive roots. These are $\omega_{c1} = 13.1187$, $\omega_{c2} = 11.0473$, and $\omega_{c3} = 2.5140\,rad/s$. The corresponding delay margins and root tendencies (RTs) are computed as $\tau_1* = 0.0786\,s$, $\tau_2* = 0.3320\,s$, $\tau_3* = 0.4958\,s$, and $RT_1 = +1, RT_2 = -1$, $RT_3 = +1$, respectively.

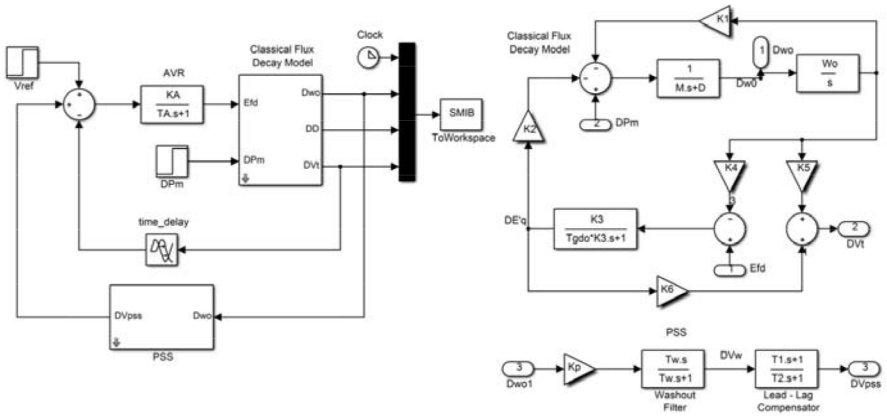

Figure 7. MATLAB/Simulink model of the SMIB system with AVR and PSS.

These results indicate that the system is stable when the delay is less than $\tau_1* = 0.0786\,s$. Since $RT_1 = +1$, a pair of the stable complex conjugate roots of Eq. (2) moves in the left half of the complex plane and crosses the imaginary axis at $s = \pm j\omega_{c1} = \pm j13.1187 rad/s$ for $\tau_1* = 0.0786\,s$, passing to the right half-plane. Therefore, the system becomes unstable for $\tau > \tau_1* = 0.0786\,s$. A simulation result illustrating this case is shown in Figure 8 for 3 different delay values ($\tau = 0.07\ s, \tau = 0.0786s$, and $\tau = 0.085s$). When the time delay is further increased, the unstable complex conjugate roots of Eq. (2) move in the right half-plane and cross the imaginary axis at $s = \pm j\omega_{c2} = \pm j11.0473 rad/s$ for $\tau_2* = 0.3320\,s$, passing to the left half-plane since the corresponding root tendency is negative, $RT_2 = -1$. Please note that the system is unstable for $\tau_1* = 0.0786\,s < \tau < \tau_2* = 0.3320\,s$. It then becomes stable again for $\tau > \tau_2* = 0.3320\,s$. Figure 9 depicts simulation results for terminal voltage around $\tau_2* = 0.3320\,s$, clearly illustrating this stability exchange from unstable to stable with an increase in time delay. Please note that the system is first unstable for $\tau = 0.32s$, then marginally stable for $\tau_2* = 0.3320\,s$, and then it becomes stable for $\tau = 0.35s$. Finally, if we continue to increase the time delay, a pair of the stable complex conjugate roots of Eq. (2) moves in the left half of the complex plane and crosses the imaginary axis at $s = \pm j\omega_{c3} = \pm j2.5140 rad/s$ for $\tau_3* = 0.4958\,s$, passing to the right half-plane since the corresponding root tendency is positive, $RT_3 = +1$. Therefore, the system becomes unstable for $\tau > \tau_3* = 0.4958\,s$ and remains unstable if the delay is further increased. A simulation result illustrating this case is shown in Figure 10 for 3 different delay values, $\tau = 0.48\ s, \tau = 0.4958s$, and $\tau = 0.51s$.

It is expected that the measurement delay observed in speed deviation in the PSS loop, which has been neglected in theoretical delay margin computation, will adversely affect stability and will reduce the delay margin. For this reason, simulation studies are carried out for the case when equal amounts of delay are

introduced into both voltage and speed deviation loops. Figures 11a and 11b show the terminal voltage for $\tau = 0.0786\,s$, $\tau = 0.02255\,s$, and $\tau = 0.024\,s$, respectively. It is clear from Figure 11a that when the same amount of delay ($\tau = 0.0786\,s$) is added to both loops, the system becomes unstable. As seen from Figure 8, the excitation control system is marginally stable at $\tau = 0.0786\,s$ when the delay in the PSS loop is not taken into account. With an additional delay in the PSS loop, the system becomes marginally stable at a lower delay value, $\tau = 0.02255\,s$, as shown in Figure 11b. As a result, the delay margin is reduced from $\tau = 0.0786\,s$ to $\tau = 0.02255\,s$.

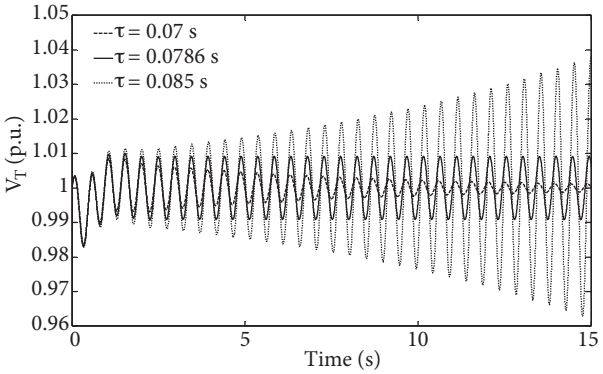

Figure 8. Generator terminal voltage for different time delays for $K_P = 20$ delay values around $\tau_1* = 0.0786\,s$ for $P_L = 0.5pu$.

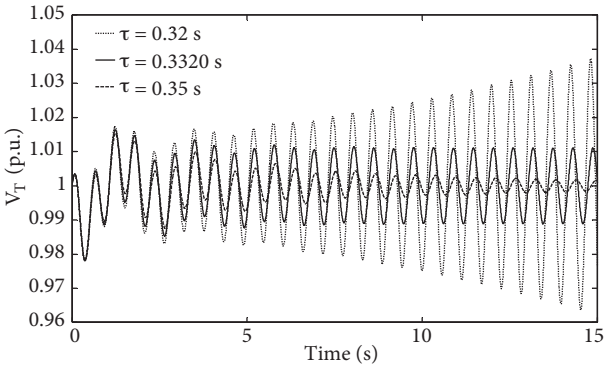

Figure 9. Generator terminal voltage for different time delays for $K_P = 20$ and delay values around $\tau_2* = 0.3320\,s$ for $P_L = 0.5pu$.

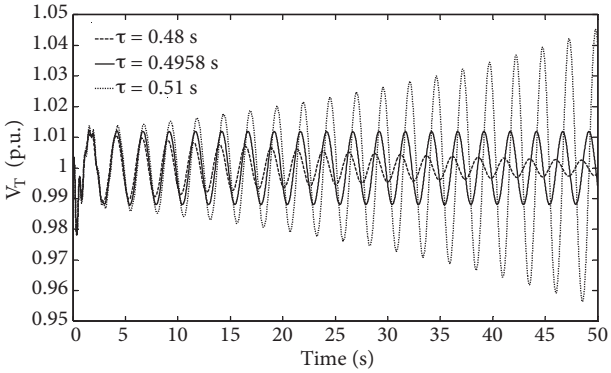

Figure 10. Generator terminal voltage for different time delays for $K_P = 20$ and delay values around $\tau_3* = 0.4958\,s$ when D = 0 and $P_L = 0.5pu$.

5. Conclusions

This paper has investigated the impact of loading and PSS gain on the stability of the generator excitation control system including a PSS with respect to the time delay using an analytical method. A useful formula is developed to compute delay margins for stability. Delay margins are computed for a wide range of PSS gain and load values. It is observed that the delay margin decreases with an increase in PSS gain and system load demand. Time-domain simulations clearly indicate that the proposed method correctly estimates delay margins. Finally, it is observed that the maximum loadability of the system decreases when time delays are taken into account in stability analysis. Together with the maximum loading point, delay margins should be used as a stability index to measure the degree of stability and to determine stability margins.

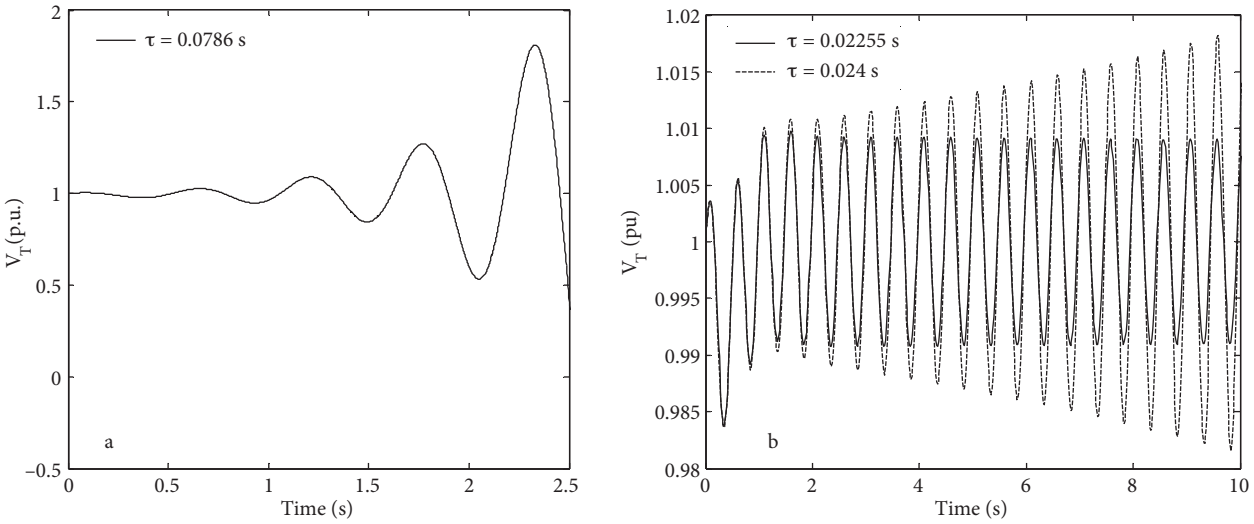

Figure 11. Generator terminal voltage for $K_P = 20$, D = 0, and $P_L = 0.5pu$ when a delay is added into PSS loop.

As future work, the proposed method will be extended to multimachine power systems whose dynamics are described by ordinary differential or differential-algebraic equations. To do that, load buses should be eliminated and a linear time-delayed state-space equation model around an operating point should be obtained. Moreover, an additional delay, which is different from the delay in the voltage control loop, will be added to the PSS loop, and delay margins will be computed using the Rekasius substitution method.

References

[1] Naduvathuparambil B, Valenti MC, Feliachi A. Communication delays in wide area measurement systems. In: Proceedings of the 34th Southeastern Symposium on System Theory; 18–19 March 2002; Huntsville, Alabama. Piscataway, NJ, USA: IEEE. pp. 118-122.

[2] Xia X, Xin Y, Xiao J, Wu J, Han Y. WAMS applications in Chinese power systems. IEEE Power Energy M 2006; 4: 54-63.

[3] Wu H, Tsakalis K, Heydt GT. Evaluation of time delay effects to wide-area power system stabilizer design. IEEE T Power Syst 2004; 19: 1935-1941.

[4] Ayasun S, Gelen A. Stability analysis of a generator excitation control system with time delays. Electr Eng 2010; 91: 347-355.

[5] Ayasun S. Computation of time delay margin for power system small-signal stability. Euro Trans Electr Power 2009; 19: 949-968.

[6] Saadat H. Power System Analysis. New York, NY, USA: McGraw-Hill, 1999.

[7] Kundur P. Power System Stability and Control. New York, NY, USA: McGraw-Hill, 1994.

[8] Sauer PW, Pai MA. Power System Dynamics and Stability. 1st Indian Reprint. Singapore: Stipes Publishing, 2002.

[9] Phadke AG. Synchronized phasor measurements in power systems. IEEE Comput Appl Pow 1993; 6: 10-15.

[10] Liu M, Yang L, Gan D, Wang D, Gao F, Chen Y. The stability of AGC systems with commensurate delays. Euro Trans Electr Power 2007; 17: 615-627.

[11] Jiang L, Yao W, Wu QH, Wen JY, Cheng SJ. Delay-dependent stability for load frequency control with constant and time-varying delays. IEEE T Power Syst 2012; 27: 932-941.

[12] Yao W, Jiang L, Wu QH, Wen JY, Cheng SJ. Wide-area damping controller of FACTS devices for inter-area oscillations considering communication time delays. IEEE T Power Syst 2014; 29: 318-329.

[13] Walton KE, Marshall JE. Direct method for TDS stability analysis. IEE Proc-D 1987; 134: 101-107.

[14] Rekasius ZV. A stability test for systems with delays. In: Proceedings of the Joint Automatic Control Conference; 13–15 August 1980; San Francisco, CA, USA. New York, NY, USA: American Society of Mechanical Engineers.

[15] Olgaç N, Sipahi R. An exact method for the stability analysis of time-delayed linear time-invariant (LTI) systems. IEEE T Autom Control 2002; 47: 793-797.

[16] He Y, Wang QG, Xie LH, Lin C. Further improvement of free-weighting matrices technique for systems with time-varying delay. IEEE T Autom Control 2007; 52: 293-299.

[17] Wu M, He Y, She JH, Liu GP. Delay-dependent criterion for robust stability of time-varying delay systems. Automatica 2004; 40: 1435-1439.

[18] Xu SY, Lam J. On equivalence and efficiency of certain stability criteria for time-delay systems. IEEE T Autom Control 2007; 52: 95-101.

[19] Yao W, Jiang L, Wu QH, Wen JY, Cheng SJ. Delay-dependent stability analysis of the power system with a wide-area damping controller embedded. IEEE T Power Syst 2011; 26: 233-240.

[20] Sönmez Ş, Ayasun S, Nwankpa CO. An exact method for computing delay margin for stability of load frequency control systems with constant communication delays. IEEE Trans Power Syst 2016; 31: 370-377.

[21] Ayasun S. Stability analysis of time-delayed DC motor speed control systems. Turk J Elec Eng Comp Sci 2013; 21: 381-393.

[22] Jalili N, Olgac N. Multiple delayed resonator vibration absorbers for multi-degree-of-freedom mechanical structures. J Sound Vib 1999; 223: 567-585.

[23] Filipovic D, Olgac N. Delayed resonator with speed feedback-design and performance analysis. Mechatronics 2002; 12: 393-413.

[24] Ji JC. Stability and bifurcation in an electromechanical system with time delays. Mech Res Commun 2003; 30: 217-225.

[25] Yan XP, Li WT. Hopf bifurcation and global periodic solutions in a delayed predator-prey system. Appl Math Comput 2006; 177: 427-445.

[26] Yan XP, Chu YD. Stability and bifurcation analysis for a delayed Lotka–Volterra predator–prey system. J Comput Appl Math 2006; 196: 198-210.

[27] Song Y, Peng Y. Stability and bifurcation analysis on a logistic model with discrete and distributed delays. Appl Math Comput 2006; 181: 1745-1757.

[28] Shahgholian G, Faiz J. The effect of power system stabilizer on small-signal stability in single-machine-infinite-bus. International Journal of Electrical and Power Engineering 2010; 4: 45-53.

[29] Falehi AL, Rostami M, Doroudi A, and Ashrafian A. Optimzayion and coordination of SVC-based supplementary controllers and PSSs to improve power system stability using a genetic algorithm. Turk J Elec Eng Comp Sci 2012; 20: 639-654.

[30] Sönmez Ş, Ayasun S, Eminoğlu U. Computation of time delay margins for stability of a single-area load frequency control system with communication delays. WSEAS Trans Power Syst 2014; 9: 67-76.

[31] Fazelina H, Sipahi R, Olgaç N. Stability robustness analysis of multiple time-delayed systems using building block concept. IEEE T Autom Control 2007; 52: 799-810.

[32] Liu Z, Zhu C, Miao Y, Jiang Q. Stability analysis of multiple time delayed power systems using building block concept. In: Proceedings of 2008 IEEE Power Engineering Society General Meeting; 20–24 July 2008; Pittsburgh, PA, USA. Piscataway, NJ, USA: IEEE. pp. 1-8.

[33] MathWorks Inc. Simulink. Model-Based and System-Based Design: Using Simulink. Natick, MA, USA: MathWorks, 2000.

Appendix

The coefficients of $P(s)$ and $Q(s)$ polynomials in Eq. (2) are given as follows:

$$p_6 = T_A T'_{d0} T_w M \omega_0 T_2$$

$$p_5 = T'_{d0} T_w M \omega_0 T_2 + K_3 T_A T_w M \omega_0 T_2 + T_A T'_{d0} M \omega_0 T_2 + T'_{d0} T_w D M \omega_0 T_2 + T_A T'_{d0} T_w M \omega_0$$

$$\begin{aligned} p_4 = {} & K_3 T_w M \omega_0 T_2 + T'_{d0} M \omega_0 T_2 + T'_{d0} T_w D \omega_0 T_2 + T'_{d0} T_w M \omega_0 + K_3 T_A M \omega_0 T_2 + K_3 T_A T_w D \omega_0 T_2 + \\ & K_3 T_A T_w M \omega_0 + T_A T'_{d0} D \omega_0 T_2 + T_A T'_{d0} M \omega_0 + T_A T'_{d0} T_w D \omega_0 + K_1 T_2 T_A T_w T'_{d0} \omega_0^2 \end{aligned}$$

$$\begin{aligned} p_3 = {} & K_3 M \omega_0 T_2 + K_3 T_w T_2 D \omega_0 + K_3 T_w M \omega_0 + T_2 T'_{d0} D \omega_0 + T'_{d0} M \omega_0 + T'_{d0} T_w D \omega_0 + K_3 D T_A T_2 \omega_0 + \\ & K_3 T_A M \omega_0 + K_3 T_A T_w D \omega_0 + T_A T'_{d0} D \omega_0 + K_1 T_2 T_A T'_{d0} \omega_0^2 + K_1 T_w T_A T'_{d0} \omega_0^2 + K_1 T_2 T_w T'_{d0} \omega_0^2 + \\ & K_1 K_3 T_2 T_w T_A \omega_0^2 + K_2 K_P K_A T_1 T_w \omega_0 - K_4 K_2 T_2 T_w T_A \omega_0^2 \end{aligned}$$

$$\begin{aligned} p_2 = {} & K_3 T_2 D \omega_0 + K_3 M \omega_0 + K_3 T_w D \omega_0 + T'_{d0} D \omega_0 + K_3 D T_A \omega_0 + K_1 T_A T'_{d0} \omega_0^2 + \\ & K_1 T_2 T'_{d0} \omega_0^2 + K_1 K_3 T_2 T_A \omega_0^2 + K_1 T_w T'_{d0} \omega_0^2 + K_1 K_3 T_w T_A \omega_0^2 + K_1 K_3 T_2 T_w \omega_0^2 + \\ & K_2 K_P K_A T_w \omega_0 - K_4 K_2 T_2 T_A \omega_0^2 - K_4 K_2 T_w T_A \omega_0^2 - K_4 K_2 T_2 T_w \omega_0^2 \end{aligned}$$

$$\begin{aligned} p_1 = {} & K_3 D \omega_0 + K_1 \omega_0^2 T'_{d0} + K_1 \omega_0^2 K_3 T_A + K_1 (\omega_0^2) T_2 K_3 + K_1 \omega_0^2 T_w K_3 - K_4 K_2 \omega_0^2 T_A - \\ & K_4 K_2 \omega_0^2 T_2 - K_4 K_2 \omega_0^2 T_w \end{aligned}$$

$$p_0 = K_1 \omega_0^2 K_3 - K_4 K_2 \omega_0^2$$

$$q_4 = K_6 K_A M T_2 T_w \omega_0$$

$$q_3 = K_6 K_A D T_2 T_w \omega_0 + K_6 K_A M T_2 \omega_0 + K_6 K_A T_w M \omega_0$$

$$q_2 = K_6 K_A M \omega_0 + K_6 K_A D T_2 \omega_0 + K_6 K_A D T_w \omega_0 + K_1 K_6 K_A T_2 T_w \omega_0^2 - K_2 K_5 K_A T_2 T_w \omega_0^2$$

$$q_1 = K_6 K_A D \omega_0 + K_1 K_6 K_A T_2 \omega_0^2 + K_1 K_6 K_A T_W \omega_0^2 - K_2 K_5 K_A T_2 \omega_0^2 - K_2 K_5 K_A T_w \omega_0^2$$

$$q_0 = K_1 K_6 K_A \omega_0^2 - K_2 K_5 K_A \omega_0^2.$$